# Interpretation of some $(p,n)$, $(n,p)$, and $(^3He, p)$ reactions by means of the statistical multistep compound emission theory

R. Bonetti, L. Colli Milazzo, and M. Melanotte
*Istituto di Fisica dell'Università di Milano, Milano, Italy*
(Received 6 July 1982)

A number of $(p,n)$, $(n,p)$, and $(^3He, p)$ reactions have been interpreted on the basis of the statistical multistep compound emission mechanism. Good agreement with experiment is found both in spectrum shape and in the value of the coherence widths.

NUCLEAR REACTIONS $^{25}Mg(^3He,p)$, $^{27}Al(^3He,p)$, $^{40}Ca(n,p)$, $^{59}Co(p,n)$, $^{89}Y(p,n)$, $^{103}Rh(p,n)$, $E_{inc}=13$, 13, 14.5, 14.7, 14.8, 18 MeV. Statistical multistep compound emission mechanism. Calculated differential cross sections and coherence widths.

## I. INTRODUCTION

In previous work[1-3] the presence of the statistical multistep compound emission (SMCE) mechanism[4] was shown in some reactions initiated by a $^3He$ beam. The aim of this paper is to extend calculations based on the SMCE mechanism to a number of reactions taken from the literature; first, to ascertain whether this effect can explain the experimental characteristics of the reactions considered and second, to extract from the comparison the values of the fundamental parameters of the theory.

It should be recalled that due to the statistical assumptions underlying this theory the angular distributions predicted are isotropic or symmetric to 90°. For this purpose we have taken from the literature only reactions showing experimental characteristics that satisfy the above conditions. It is worth pointing out that these conditions are found more easily among reactions induced by low energy projectiles which make possible the formation of bound states along the precompound chain and therefore assure the consequent validity of the statistical assumptions on which the SMCE theory is based.

The reactions considered here are the following: $^{25}Mg(^3He,p)$,[1] $^{27}Al(^3He,p)$,[2] $^{40}Ca(n,p)$,[5] $^{59}Co(p,n)$,[6] $^{89}Y(p,n)$,[7] and $^{103}Rh(p,n)$.[8] The excitation energies (see Table I) range from a minimum of about 20 MeV to a maximum of about 35 MeV.

## II. DESCRIPTION OF THE METHOD OF ANALYSIS

The calculations described herein essentially follow the formulation of the SMCE theory developed by Feshbach *et al.*[4] According to this theory the formula for the cross section reads as follows:

TABLE I. Comparison between calculated and experimental values for the $r$-stage width $\langle\Gamma_r\rangle$.

| Composite nucleus | Result of calculations | $\langle\Gamma_r\rangle$ (keV) Experimental values |
|---|---|---|
| $^{28}Si$ | 42 ($E_{exc}=36$ MeV) | 50 ±10 ($E_{exc}=36$ MeV) Ref. 3 |
| | | 110 ±15 ($E_{exc}=30$ MeV) Ref. 19 |
| $^{30}P$ | 85 ($E_{exc}=31$ MeV) | 55 ±11 ($E_{exc}=31$ MeV) Ref. 20 |
| | | 73 ±10 ($E_{exc}=20$ MeV) Ref. 16 |
| $^{41}Ca$ | 24 ($E_{exc}=23$ MeV) | 10 ±5 ($E_{exc}=19$ MeV) Ref. 16 |
| $^{60}Ni$ | 10 ($E_{exc}=24$ MeV) | 5 ±2 ($E_{exc}=20$ MeV) Ref. 16 |
| $^{90}Zr$ | 0.38 ($E_{exc}=23$ MeV) | 0.173±0.087 ($E_{exc}=21$ MeV) Ref. 16 |
| $^{104}Pd$ | 3.34 ($E_{exc}=27$ MeV) | 0.233±0.064 ($E_{exc}=18$ MeV) Ref. 16 |

 

$$\frac{d^2\sigma}{d\Omega\, d\epsilon}=\pi\lambda^2\sum_J(2J+1)\left[\sum_{N=1}^{r}\left\{\sum_{\nu=N-1}^{N+1}\sum_{ls\lambda}C^{\lambda}_{lsJ}P_\lambda(\cos\vartheta)\frac{\langle\Gamma^{\uparrow ls\nu}_{NJ}(U)\rho_{J\nu}(U)\rangle}{\langle\Gamma_{NJ}\rangle}\right\}\left[\prod_{m=1}^{N-1}\frac{\langle\Gamma^{\downarrow}_{mJ}\rangle}{\langle\Gamma_{mJ}\rangle}\right]\right]2\pi\frac{\langle\Gamma^{\rm in}_{1J}\rangle}{\langle D_{1J}\rangle}\ , \tag{1}$$

where

$$\langle\Gamma_N\rangle=\langle\Gamma^{\downarrow}_N\rangle+\langle\Gamma^{\uparrow}_N\rangle$$

is the average total width of an $n$-exciton state ($n=2N+1$) in the weak coupling approximation.

A few improvements were introduced into the application of the theory. Most of them have already been described in a previous paper,[9] where the value of the quantity $\langle\Gamma^{\downarrow}_N\rangle$ (damping width) as experimentally extracted from fluctuation measurements was calculated. The first modification concerns the Ericson formulas for the $n$-exciton level densities, where the binding energies of the nucleons in the various composite nuclei are taken as the maximum possible value for the energy of the excited particles. This is done because the SMCE theory assumes a chain of stages in which all the excited particles must be in bound states.

The other change is in the calculation of the matrix elements of the residual potential, needed to construct the damping and escape widths $\langle\Gamma^{\downarrow}_N\rangle$ and $\langle\Gamma^{\uparrow}_N\rangle$. These widths are proportional to the square of the overlap integrals of the radial wave functions $u_j$ which describe the interacting particles at each step of the chain:

$$\vartheta=V_0(\tfrac{4}{3}\pi r_0{}^3)\frac{1}{4\pi}\int_0^\infty u_{j_1}u_{j_2}u_l u_{j_3}\frac{dr}{r^2}\ . \tag{2}$$

The above expression was obtained with a zero-range form of the two-body residual interaction. The strength of this interaction, $V_0$, can be fixed by reproducing both the value of the total width of a particular $n$-exciton state, as extracted from fluctuation experiments, and the absolute values of cross sections of reactions having the peculiar characteristics predicted by the SMCE mechanism.

Previous work done along both these lines[2,3,18] led to results for $V_0$ that were consistent but too low: Comparison with values extracted from nuclear structure and direct reaction work shows a discrepancy of at least one order of magnitude.[10–12] This was mainly due to the fact that in the early evaluations of expression (2), in order to simplify calculations very rough wave functions were used. In fact they were all taken as constant within the nuclear volume and independent of the $j$ value of the orbits involved. This, of course, maximized the overlap integrals and consequently minimized the value of $V_0$ necessary to reproduce the experimental data.

In the current calculations we have described both bound and unbound excited particles by means of realistic wave functions. For bound excited particles we used harmonic oscillator wave functions, after having checked their practical identity in the mass range examined with the Saxon-Woods functions. Unbound excited particles present in the entrance and exit channels have been described by the usual distorted wave functions obtained by means of the optical model. To calculate these wave functions we used the well-known parameters of Becchetti and Greenlees[13] for the medium-heavy targets and of Perey and Perey[14] for the light targets ($^{25}$Mg and $^{27}$Al). Throughout the calculations we disregarded the spin of the incoming and outgoing particles.

For the choice of the quantum numbers for bound particles we based our approach essentially on the shell model, while keeping in mind that the single particle shell model cannot be strictly valid for the nuclei studied here owing to the probable presence of distortion and pairing effects. We therefore included in the calculations a greater number of orbits than would be given by the strict single particle model, to make sure that all the significant $l$ values

TABLE II. Calculated entrance width $2\pi\langle\Gamma^{\rm in}_J\rangle/D$ as a function of $J$ for the nucleon induced reactions.

| | Entrance widths $2\pi\frac{\langle\Gamma^{\rm in}\rangle}{D}$ | | | | | |
|---|---|---|---|---|---|---|
| Reaction | $J=0$ | $J=1$ | $J=2$ | $J=3$ | $J=4$ | $J=5$ |
| $^{40}$Ca$(n,p)$ | 0.742 | 1.021 | 0.750 | 0.314 | 0.014 | 0.013 |
| $^{59}$Co$(p,n)$ | 1.026 | 1.174 | 0.726 | 0.205 | 0.009 | 0.011 |
| $^{89}$Y$(p,n)$ | 0.352 | 0.280 | 1.115 | 1.168 | 0.216 | 0.016 |
| $^{103}$Rh$(p,n)$ | 0.104 | 0.035 | 0.033 | 0.377 | 0.612 | 0.149 |

present in the entrance channel contribute to the construction of the various widths. In the reactions considered here, the fairly low energy of the incoming particles and the consequent behavior as a function of $l$ of the transmission coefficients and the entrance widths [the term $2\pi\langle\Gamma^{\text{in}}\rangle/D$ in formula (1)] made us realize that a substantial contribution to the cross section is given only by the first six $l$ values.

This is also confirmed by the behavior of the function $R(J)$, the spin distribution function of the levels [see formula (5.7) of Ref. 4], whose value drops rapidly when $l$ increases.

We want to point out that in the case of the $(p,n)$ and $(n,p)$ reactions the complete expression for the SMCE cross section (1) was calculated, including the entrance width $2\pi(\langle\Gamma^{\text{in}}\rangle/D)$.

In fact, in these reactions it was supposed that the first stage of the chain was formed of three excitons, and this makes microscopic calculation of the entrance width manageable.[15] When considering $^3$He induced reactions instead, as in previous work,[1-3] it

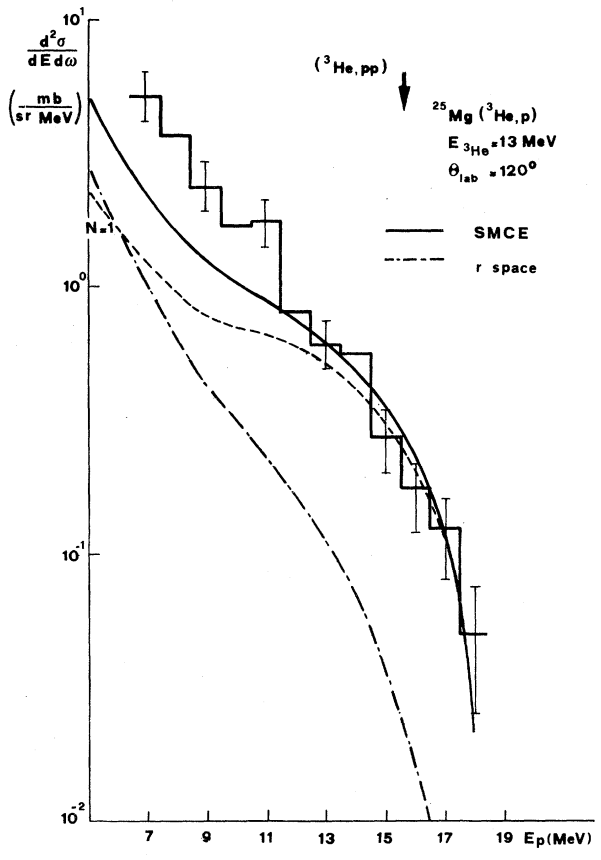


FIG. 1. Experimental and calculated spectra at backward angles for the various reactions. The arrows indicate the thresholds of some multiple reactions.

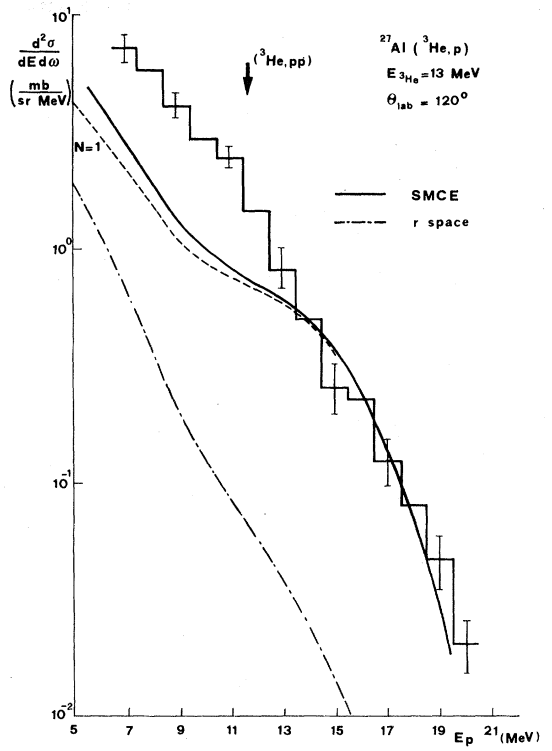


FIG. 2. Experimental and calculated spectra at backward angles for the various reactions. The arrows indicate the thresholds of some multiple reactions.

turns out that $^3$He breaks up into its components, thus making the first a five-exciton stage. In this case microscopic calculation of the entrance width is quite complicated, and we prefer to use the well-known relation

$$T_J \simeq 2\pi \frac{\langle\Gamma_J^{\text{in}}\rangle}{D} .$$

The behavior of the term $2\pi(\langle\Gamma_J^{\text{in}}\rangle/D)$ as a function of $J$ for the various reactions is shown in Table II. It is worth pointing out that due to the improvements introduced into the application of the theory and particularly to the saturation of the level densities with increasing energy (due, as previously stated, to the upper limit imposed to the excited particles by the binding energy), the entrance widths do not change significantly in the mass and excitation energy range examined, remaining always approximately $\leq 1$.

The present calculation is thus the first example of a complete comparison of the experiments with the predictions based on the SMCE theory that was made using realistic level density functions and realistic wave functions for the descriptions of the interacting particles.

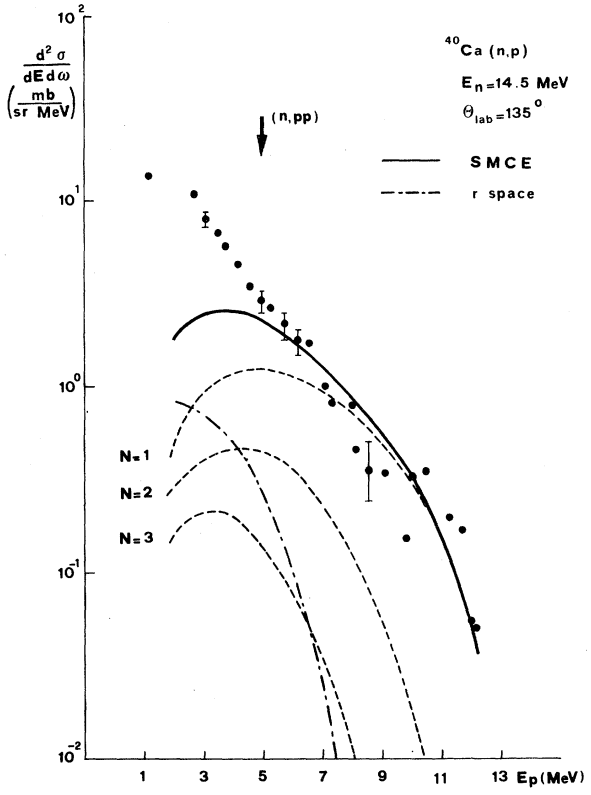


FIG. 3. Experimental and calculated spectra at backward angles for the various reactions. The arrows indicate the thresholds of some multiple reactions.

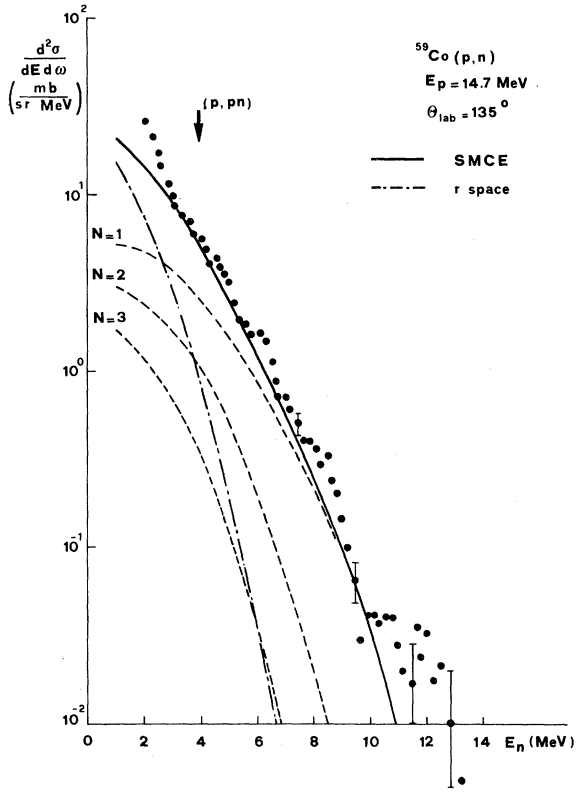


FIG. 4. Experimental and calculated spectra at backward angles for the various reactions. The arrows indicate the thresholds of some multiple reactions.

## III. RESULTS AND COMPARISON WITH THE EXPERIMENTS

Figures 1–6 show a comparison of the calculations described above with the spectra of protons from $^{25}Mg(^3He,p)$, $^{27}Al(^3He,p)$, and $^{40}Ca(n,p)$ and of neutrons from $^{59}Co(p,n)$, $^{89}Y(p,n)$, and $^{103}Rh(p,n)$. All these spectra were emitted in a backward direction (120°, 135°, or 145°). As already stated, the angular distributions of the emitted particles were found to be symmetric to 90° or, at worst, flat in the backward part [this is particularly the case of the reaction $^{103}Rh(p,n)$ (Ref. 8)].

In each figure the contribution from the various stages of the precompound chain is indicated, together with the contribution of the evaporation $r$

TABLE III. Parameters used in the calculations: $V_0$, the strength of the residual two-body interaction (in MeV); $a_c$, the single-particle level density parameter of the composite nucleus (from Ref. 17) (in $MeV^{-1}$); $a_{R1}$, the same as $a_c$ but for the residual nucleus; $a_{R2}$, the same as $a_c$ but for the residual nucleus of the reaction in competition; $R_0$, the nuclear radius parameter (in fm); and $\sigma$, the spin cutoff parameter.

| Reaction | $V_0$ | $a_c$ | $a_{R1}$ | $a_{R2}$ | $R_0$ | $\sigma$ |
|---|---|---|---|---|---|---|
| $^{25}Mg(^3He,p)$ | 5 | 3 | 3.5 | 3 | 1.2 | 2.4[a] |
| $^{27}Al(^3He,p)$ | 5 | 3 | 4 | 3 | 1.2 | 2.4[a] |
| $^{40}Ca(n,p)$ | 5 | 5.59 | 5.5 | 5 | 1.2 | 1.9 |
| $^{59}Co(p,n)$ | 5 | 8 | 8 | 7 | 1.2 | 2.2 |
| $^{89}Y(p,n)$ | 5 | 12 | 10 | 9 | 1.2 | 2.6 |
| $^{103}Rh(p,n)$ | 5 | 14.5 | 15 | 15 | 1.2 | 2.7 |

[a]These values of the spin cutoff parameter are slightly higher than those calculated according to the prescriptions of Ref. 4 owing to the distortion of the nuclei involved.

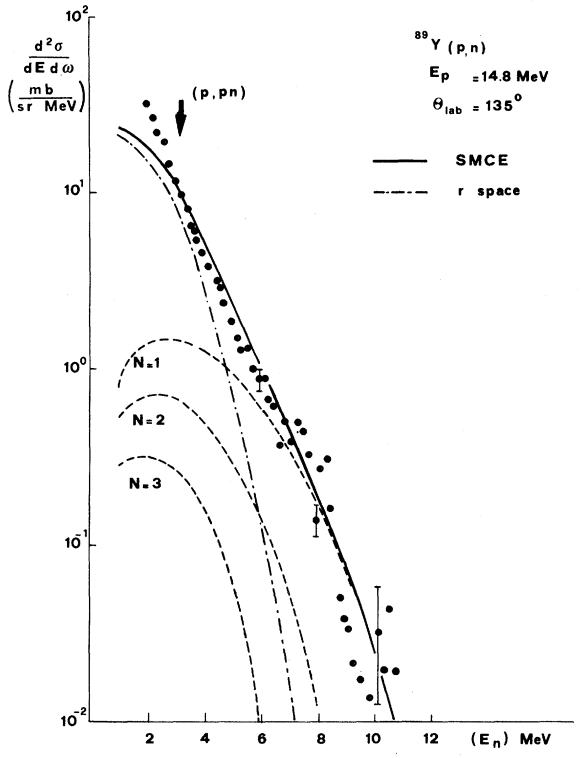


FIG. 5. Experimental and calculated spectra at backward angles for the various reactions. The arrows indicate the thresholds of some multiple reactions.

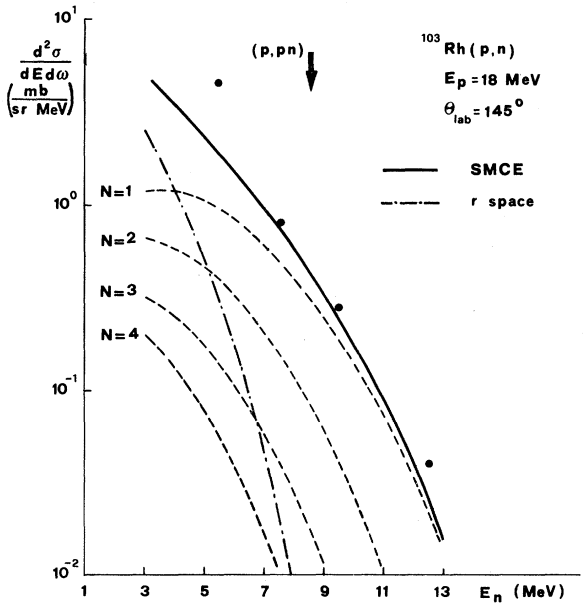


FIG. 6. Experimental and calculated spectra at backward angles for the various reactions. The arrows indicate the thresholds of some multiple reactions.

stage. In the case of $^3$He induced reactions, only one stage, the five-exciton one, contributes before equilibrium is reached, while in the reactions initiated by nucleons, due also to the higher mass number, three or four stages contribute before the equilibrium. This has been evaluated according to the condition given in Ref. 4; that is, a stage is considered as belonging to the precompound chain and is thus not included in the equilibrium $r$ stage as long as its level density value $\rho_N$ is at least ten times smaller than that of the next stage.

In all the cases shown, the calculations underevaluate the experiments in the lowest energy part of the emitted particle spectrum. This fact can be explained by the probable presence of some multiple reactions. In the particular case of the $^{27}$Al($^3$He,$p$) reaction, there is probably also a deuteron component not completely eliminated by the experimental equipment.

The parameters used in the calculations are indicated in Table III. It is worth pointing out the constancy of the fundamental parameter $V_0$ of the two-

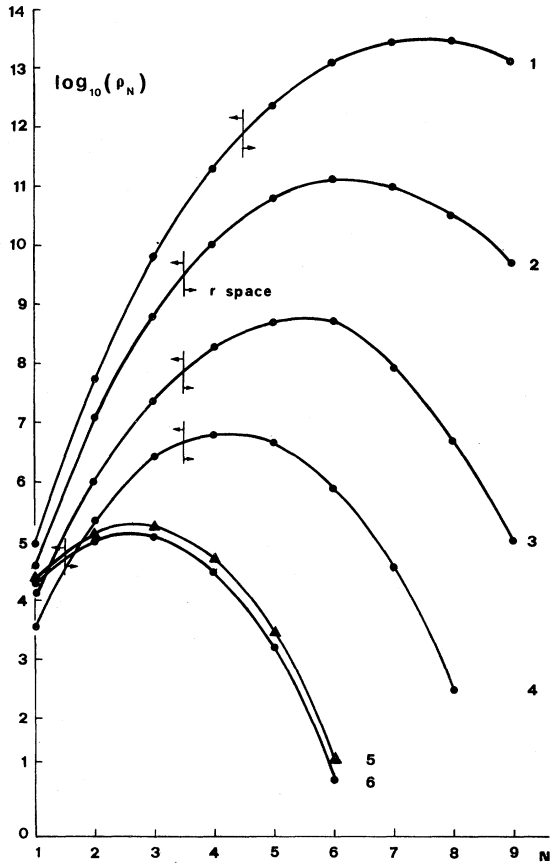


FIG. 7. Level density of the various composite nuclei as a function of the stage $N$ of the precompound chain: (1) $^{104}$Pd, (2) $^{90}$Zr, (3) $^{60}$Ni, (4) $^{41}$Ca, (5) $^{30}$P, and (6) $^{28}$Si.

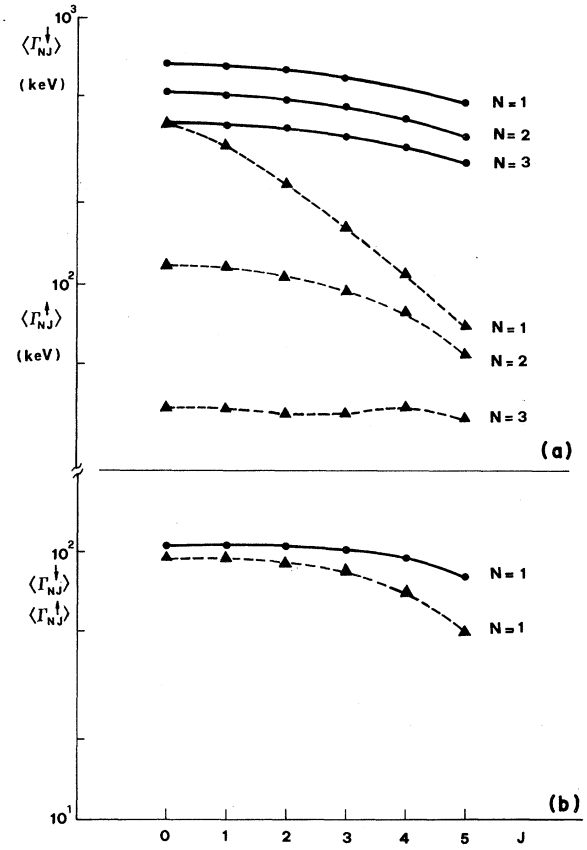


FIG. 8. Damping ($\langle\Gamma_{NJ}^{\downarrow}\rangle$, solid line) and escape ($\langle\Gamma_{NJ}^{\uparrow}\rangle$, dashed line) widths as a function of $J$ in the case of (a) $^{40}$Ca($n$,$p$) and (b) $^{25}$Mg($^3$He,$p$).

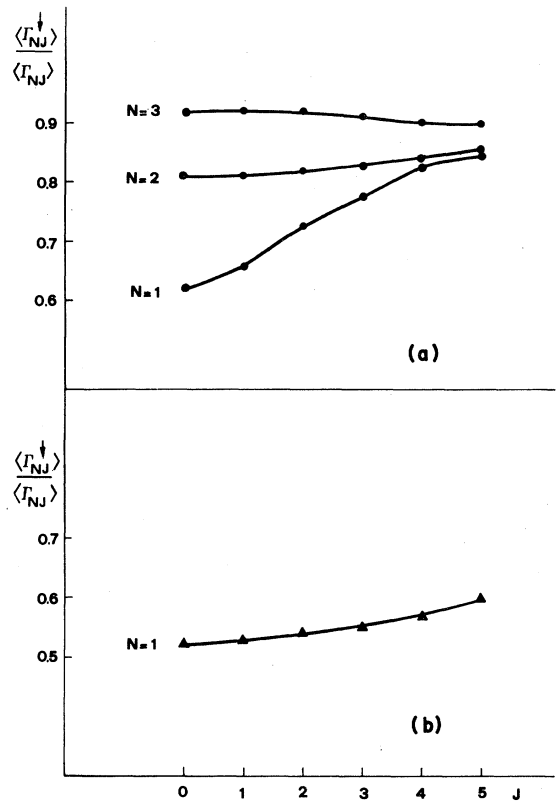


FIG. 9. Transmission probability $\langle\Gamma_{NJ}^{\downarrow}\rangle/\langle\Gamma_{NJ}\rangle$ as a function of $J$ in the case of (a) $^{40}$Ca($n$,$p$) and (b) $^{25}$Mg($^3$He,$p$).

body interaction, taken with the shape of a $\delta$ function

$$V = V_0(\tfrac{4}{3}\pi r_0^3)\delta(r_1 - r_2)\ ,$$

which turns out to be 5 MeV (or about 36 MeV fm$^3$ when expressed, as commonly done in many papers, as $V_0$ multiplied by the elementary volume).

This value is not far from the one used in many nuclear structure calculations done with the same residual interaction shape. For instance, in Ref. 10 a maximum value of about 60 MeV fm$^3$ is given in the surface region, where the interaction is considerably stronger than in the inner part of the nucleus.

TABLE IV. Comparison between calculated and experimental values for the five-exciton stage width $\langle\Gamma_5\rangle$ of the $^3$He induced reactions.

| Composite nucleus | $\langle\Gamma_5\rangle$ calc (keV) | $\langle\Gamma_5\rangle$ expt (keV) | Ref. |
|---|---|---|---|
| $^{28}$Si | 230 | 220±44 | 3 |
| $^{30}$P | 220 | 230±46 | 2 |

Figure 7 shows the behavior of the level density as a function of the stage $N$ for the various composite nuclei studied.

Figure 8 shows the values of $\langle\Gamma_{NJ}^{\downarrow}\rangle$, the damping width, and $\langle\Gamma_{NJ}^{\uparrow}\rangle$, the escape width, for the various stages along the chain and for different angular mo-

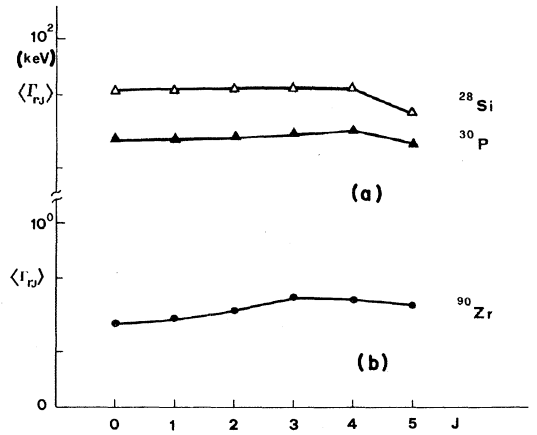


FIG. 10. Behavior of the $r$-stage width $\langle\Gamma_{rJ}\rangle$ as a function of $J$ for some composite nuclei.

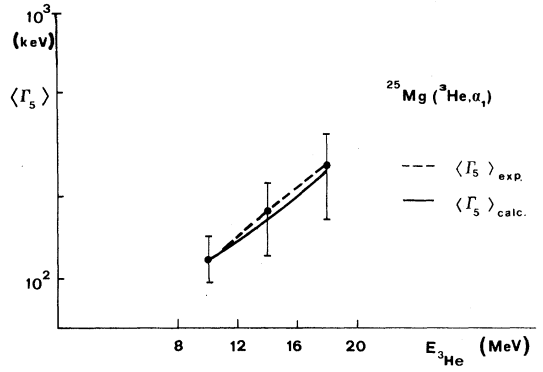


FIG. 11. Comparison between experimental and calculated values of the five-exciton stage width $\langle \Gamma_5 \rangle$ as a function of the incident energy.

menta $J$, in the two typical cases of $^{40}$Ca($n$,$p$) (the reaction in which the first stage is considered as a three-exciton one) and $^{25}$Mg($^3$He,$p$) (the reaction in which the first stage is considered as a five-exciton one). As can be seen, the damping widths decrease slowly along the chain, while the escape widths drop more rapidly, thus explaining the decreasing contribution as a function of $N$.

Figure 9 shows the transmission probability through each stage $N$ of the chain in the equilibration process,

$$\langle \Gamma_{NJ}^{\downarrow} \rangle / \langle \Gamma_{NJ} \rangle \ .$$

As $N$ increases, the escape widths diminish much more rapidly than the damping widths, so that equilibration becomes favored over emission. In Fig. 10 $\langle \Gamma_{rJ} \rangle$, the width of the composite nucleus, is plotted as a function of $J$ for some of the reactions studied.

In Table I the same quantity averaged over $J$ is shown compared with its experimentally obtained values.[3,16,19,20] It is very interesting to note that the theoretical and experimental values agree quite well when the differences in the excitation energies are taken into account. Moreover, the widths of the five-exciton stage in the case of $^3$He induced reactions are found to agree quite well with those measured experimentally[2,3] (see Table IV).

In the case of the $^{25}$Mg($^3$He,$\alpha_1$) reaction, measurement of this width over a large excitation energy interval[3] makes possible a comparison with the prediction given by the SMCE theory of $\langle \Gamma_5 \rangle$ as a function of energy. Figure 11 shows the good agreement obtained in this comparison.

## IV. CONCLUSIONS

The calculations presented in this paper confirm the validity of the SMCE theory in reproducing the experimental cross sections of reactions induced by low energy projectiles on light and medium-heavy targets.

The improvements introduced in the application of the theory make the extraction possible through comparison with the experiments of a value for the two-body residual interaction $V_0$ which is in reasonable agreement with the one given by independent calculations.

Moreover, by using this value for $V_0$ we reproduced the experimental widths connected with both the equilibrium and the first stage of the SMCE chain.

We want to point out, however, the difficulty in finding reactions whose experimental characteristics make possible their unambiguous interpretation as being due purely to the SMCE mechanism. For this reason we believe that fluctuations in the entrance channel, as pointed out in Ref. 3, should be considered a very important tool to better discriminate between the various reaction mechanisms.

## ACKNOWLEDGMENTS

We want to thank Dr. S. Perez for kindly making his code DISTWAV available to us. Thanks are also due to Professor P. Hodgson, Professor L. Lanz, and Professor P. Mello for their interest in this work and for useful suggestions.

[1]A. De Rosa, G. Inglima, E. Rosato, M. Sandoli, R. Bonetti, and L. Colli Milazzo, J. Phys. G 4, L71 (1978).
[2]R. Bonetti, L. Colli Milazzo, A. De Rosa, G. Inglima, E. Perillo, M. Sandoli, and F. Shahin, Phys. Rev. C 21, 816 (1980).
[3]R. Bonetti, L. Colli Milazzo, M. Melanotte, A. De Rosa, G. Inglima, E. Perillo, M. Sandoli, V. Russo, N. Saunier, and F. Shahin, Phys. Rev. C 25, 717 (1982).
[4]H. Feshbach, A. Kerman, and S. Koonin, Ann. Phys. (N.Y.) 125, 429 (1980).
[5]L. Colli, U. Facchini, I. Iori, G. Marcazzan, A. Sona, and M. Pignanelli, Nuovo Cimento 7, 400 (1958).
[6]S. M. Grimes, J. D. Anderson, J. W. McClure, B. A. Pohl, and C. Wong, Phys. Rev. C 3, 645 (1971).
[7]S. M. Grimes, J. D. Anderson, B. A. Pohl, J. W. McClure, and C. Wong, Phys. Rev. C 4, 607 (1971).
[8]C. Kalbach, S. M. Grimes, and C. Wong, Z. Phys. A 275, 175 (1975).
[9]R. Bonetti, L. Colli Milazzo, and M. Melanotte, Lett. Nuovo Cimento 31, 33 (1981).
[10]Z. Bochnacki, I. M. Holban, and I. N. Mikhailov, Nucl. Phys. A97, 35 (1967).
[11]J. M. Ferguson, Nucl. Phys. 59, 97 (1964).
[12]S. M. Austin, in *The (p,n) Reaction and the Nucleon-*

*Nucleon Force,* edited by C. D. Goodman, S. M. Austin, S. D. Bloom, J. Rapaport, and G. R. Satchler (Plenum, New York, 1980).
[13]F. D. Becchetti, Jr. and G. W. Greenlees, Phys. Rev. 182, 1190 (1969).
[14]C. M. Perey and F. G. Perey, At. Data Nucl. Data Tables 17, 1 (1976).
[15]H. Feshbach (private communication).
[16]M. G. Braga Marcazzan and L. Milazzo Colli, Progr. Nucl. Phys. 2, 145 (1969).
[17]U. Facchini and E. Saetta-Menichella, Energia Nucleare 15, 54 (1968).
[18]H. Feshbach, in *Proceedings of the International Conference on Nuclear Physics, Munich, 1973,* edited by J. De Boer and H. J. Mang (North-Holland, Amsterdam/American Elsevier, New York, 1973).
[19]J. D. A. Roeders, L. W. Put, A. G. Drentje, and A. Van Der Woude, Lett. Nuovo Cimento 2, 209 (1969).
[20]R. Bonetti, L. Colli Milazzo, and A. Garegnani, Lett. Nuovo Cimento 29, 496 (1980).